THE JOURNAL OF BIOLOGICAL CHEMISTRY
Vol. 279, No. 52, Issue of December 24, pp. 54264–54274, 2004
Printed in U.S.A.

Plant UBX Domain-containing Protein 1, PUX1, Regulates the Oligomeric Structure and Activity of Arabidopsis CDC48*

Received for publication, May 17, 2004, and in revised form, September 21, 2004
Published, JBC Papers in Press, October 21, 2004, DOI 10.1074/jbc.M405498200

David M. Rancour, Sookhee Park, Seth D. Knight, and Sebastian Y. Bednarek‡

From the Department of Biochemistry, University of Wisconsin-Madison, Madison, Wisconsin 53706

p97/CDC48 is a highly abundant hexameric AAA-ATPase that functions as a molecular chaperone in numerous diverse cellular activities. We have identified an Arabidopsis UBX domain-containing protein, PUX1, which functions to regulate the oligomeric structure of the Arabidopsis homolog of p97/CDC48, AtCDC48, as well as mammalian p97. PUX1 is a soluble protein that co-fractionates with non-hexameric AtCDC48 and physically interacts with AtCDC48 *in vivo*. Binding of PUX1 to AtCDC48 is mediated through the UBX-containing C-terminal domain. However, disassembly of the chaperone is dependent upon the N-terminal domain of PUX1. These findings provide evidence that the assembly and disassembly of the hexameric p97/CDC48 complex is a dynamic process. This new unexpected level of regulation for p97/CDC48 was demonstrated to be critical *in vivo* as *pux1* loss-of-function mutants display accelerated growth relative to wild-type plants. These results suggest a role for AtCDC48 and PUX1 in regulating plant growth.

The 97-kDa valosin-containing protein (p97/VCP) and its yeast ortholog, CDC48, are members of the AAA[1] family (ATPases associated with diverse cellular activities), which comprises a highly conserved and ubiquitous group of molecular chaperones (for review see Ref. 1–4). AAA proteins are characterized by the presence of one (type I) or two (type II) ATPase domains containing the Walker A and B motifs that are responsible for ATP binding and hydrolysis, respectively. The active form of many family members are ring-shaped oligomers, typically hexamers, that undergo conformational changes upon binding and hydrolysis of ATP.

p97/CDC48 is an abundant type II hexameric AAA protein that functions in numerous diverse cellular activities including homotypic fusion of endoplasmic reticulum (ER) and Golgi membranes (5–8), ER-associated protein degradation (ERAD) (9–12), nuclear envelope reassembly (13), lymphocyte stimulation (14), and cell cycle progression (15). In addition, p97/CDC48 have been found to be associated with various other proteins involved in vesicle trafficking (16, 17) and DNA replication and repair; however, its function in these pathways has not been well characterized (18–20). The ATP-driven conformational changes in p97/CDC48 are utilized most likely for protein assembly and disassembly in the various pathways.

The functional versatility of p97/CDC48 appears to be mediated by multiple adapter/regulatory proteins that dictate the substrate specificity of this molecular chaperone. In the fusion of mammalian ER and Golgi membranes, a p97/CDC48 complex containing the adapter protein, p47, interacts with the t-SNARE, syntaxin 5 (6, 8). Dissociation of p97/CDC48-p47 from syntaxin 5 has recently been shown to require an additional factor, VCIP135 (21, 22). Mammalian p97, p47, and another cofactor, the heterodimeric complex, Ufd1-Npl4, have also been found to regulate sequential steps during nuclear envelope assembly (13). In addition, p97/CDC48 functions with Ufd1-Npl4 and other members of the UFD pathway, Ufd2 (23) and Ufd3 (24) in ubiquitin-proteasome protein processing and degradation including ERAD (9, 11, 12, 25, 26). Interestingly, p97/CDC48, the p97/CDC48-p47 complex, and Ufd1-Npl4 bind mono- and/or polyubiquitin chains (12, 27, 28). It remains to be determined how their interaction with ubiquitin contributes to two seemingly distinct processes such as Golgi assembly and protein degradation.

Binding of p47, Ufd1-Npl4, and another recently identified p97/CDC48 adapter, SVIP (29), which is required for the maintenance of ER integrity, is mutually exclusive. These proteins appear bind to the N-terminal domains of p97/CDC48 thereby coupling the outside edge of the active hexameric barrel to its targets. In the case of p47, binding of the protein to the N terminus of p97/CDC48 is mediated through two contiguous sites; a C-terminal UBX domain and middle ~100 amino acid region (amino acids 171–270) of undetermined structure (30, 31).

UBX domains have been identified in a number of functionally diverse eukaryotic proteins. The domain is located typically at the C terminus. Recent work has shown that the *Saccharomyces cerevisiae* genome encodes 7 UBX-containing proteins including the putative yeast ortholog of p47, Shp1p (21), the yeast Cui1–3p protein family, which are required for sporulation (32), and proteins designated Ubx2, Ubx3, and Ubx5 (33). Similar to p47, all of the yeast UBX-containing proteins bind to CDC48 via UBX domains (32, 33). Structural studies of the UBX domain of the human Fas-associated factor-1 (FAF1) (34) and p47 (30) have shown that the UBX domain adopts a characteristic ubiquitin fold. In contrast to

* This research was supported by Grant DE-FG02-99ER20332 from the Department of Energy, Division of Energy Biosciences. The costs of publication of this article were defrayed in part by the payment of page charges. This article must therefore be hereby marked "*advertisement*" in accordance with 18 U.S.C. Section 1734 solely to indicate this fact.

The nucleotide sequence(s) reported in this paper has been submitted to the GenBank™/EBI Data Bank with accession number(s) AY572781, AY572782, AY572783, and AY572784.

‡ To whom correspondence should be addressed: Dept. of Biochemistry, University of Wisconsin-Madison, 433 Babcock Dr., Madison, WI 53706. Tel.: 608-263-0309; Fax: 608-262-3453; E-mail: bednarek@biochem.wisc.edu.

[1] The abbreviations used are: AAA, ATPase associated with diverse cellular activities; ATPaseBB, ATPase binding buffer; ER, endoplasmic reticulum; ERAD, endoplasmic reticulum-associated protein degradation; MIB, membrane isolation buffer; MS, Murashige and Skoog salts; PIC, protease inhibitor cocktail; PUX, Plant UBX-containing protein; VSC, velocity sedimentation centrifugation; IPTG, isopropyl-1-thio-β-D-galactopyranoside; AMP-PNP, adenosine 5′-(β,γ-imino)triphosphate; MALDI-TOF, matrix-assisted laser desorption/ionization-time of flight; NSF, *N*-ethylmaleimide-sensitive fusion protein; GST, glutathione *S*-transferase; DTT, dithiothreitol.

ubiquitin, the UBX domain lacks the C-terminal double glycine motif necessary for conjugation to target proteins.

Our previous studies have suggested that the plant orthologs of p97/CDC48 and another structurally related member of the AAA ATPase, the *N*-ethylmaleimide-sensitive fusion protein, NSF, function in distinct membrane fusion pathways at the plane of cell division to mediate plant cytokinesis (35). The Arabidopsis p97/CDC48 and syntaxin 5 orthologs, AtCDC48 and SYP31, respectively, were found to colocalize at the division plane during cytokinesis and to interact *in vitro* and *in vivo*. To characterize further the function of AtCDC48 and SYP31 we have utilized affinity chromatography and MALDI-MS to identify plant proteins that interact with SYP31 and/or modulate the activity of AtCDC48. Here we show that one member of the plant UBX domain-containing protein family (PUX), PUX1, regulates AtCDC48 by inhibiting its ATPase activity and by promoting the disassembly of the active hexamer. Phenotypic analysis of *pux1* plants revealed that the loss of PUX1 accelerated the growth of various plant organs including roots and inflorescence shoots. These results suggest that PUX1 functions as a regulator of AtCDC48 and that the activity of these two proteins is required for various cellular pathways important for plant growth and development.

EXPERIMENTAL PROCEDURES

Affinity Chromatography, MALDI-Mass Spectrometry, and Protein Identification—GST and GST-SYP31-(41–281ΔTM) were expressed in *Escherichia coli* and purified as before (35). Purified protein was bound to glutathione-Sepharose 4B (Amersham Biosciences, Piscataway, NJ) in Tris-buffered saline (TBS; 25 mM Tris-HCl, pH 7.4, 137 mM NaCl, 0.27 mM KCl) at 1 mg of protein per ml of bead volume. Unbound material was removed and the column washed with 10 column volumes of TBS. The protein was coupled covalently to the resin using 20 mM dimethyl pimelimidate (DMP) in 200 mM sodium borate, pH 8.8, and quenched with Tris buffer as described previously (36). The protein columns were washed extensively with TBS and stored in TBS, 0.02% sodium azide at 4 °C.

Arabidopsis T87 suspension-cultured cell cytosol (T87 S150) was prepared as described (S150′; Rancour *et al.*, Ref. 35) in $MIB^{+DTT+PIC}$ (20 mM HEPES/KOH, pH 7.0, 50 mM KOAc, 1 mM $Mg(OAc)_2$, 250 mM sorbitol, 1 mM dithiothreitol (DTT), and protease inhibitor mixture including 1 mM phenylmethylsulfonyl fluoride, 5 μg/ml pepstatin A, 1 μg/ml chymostatin, 1 mM *p*-aminobenzamidine, 1 mM ϵ-aminocaproic acid, 5 μg/ml aprotinin, 1 μg/ml leupeptin, 10 μg/ml E64). For the identification of AtCDC48/SYP31-interacting protein, immobilized GST/GST-SYP31 glutathione-Sepharose was incubated with S150 protein in binding buffer ($MIB^{+DTT+PIC}$ plus 0.1% (v/v) Nonidet P-40 and 1 mM ATP) at 4 °C for 1.5 h in 5-ml final volume at a final protein ratio of 0.25 mg of GST/GST-SYP31:13 mg of S150 protein. Bound protein complexes were collected by centrifugation of the resin and removal of unbound solution. The beads were washed with 9 ml of MIB^{DTT}+0.1% (v/v) Nonidet P-40, and the final wash solution was removed with a 27-gauge needle and syringe. Protein was eluted from the beads with MIB^{DTT}+0.1% (v/v) Nonidet P-40 + 250 mM NaCl by incubation 25 min at 22 °C and then stored at −20 °C.

Proteins were precipitated using trichloroacetic acid (10% w/v final), solubilized in 2× SDS-PAGE loading buffer, and analyzed by preparative discontinuous SDS-PAGE (4% stacking; 10% resolving). Proteins were visualized by Coomassie Blue staining. Protein bands specific to GST-SYP31 but not present in the GST control sample were excised, washed, reduced with DTT, alkylated with iodoacetamide, digested with trypsin (sequencing grade; Promega, Madison, WI), and resulting peptides eluted and dried according to Jimenez *et al.* (37). Peptides were analyzed by MALDI-TOF mass spectrometry at the University of Wisconsin-Madison Biotechnology Center. Mass peak data were analyzed using the Mascot software program (38) to identify the best-fit Arabidopsis protein matches.

Sequence Data—Sequence data for PUX1–4 have been submitted to GenBank™ under accession nos. AY572781, AY572782, AY572783, and AY572784.

PUX1 Interaction Studies with AtCDC48, Mouse p97, and Mammalian NSF Binding Assays—Mammalian His_6-p97 and His_6-NSF-myc were prepared as described (27, 39). PUX1 binding assays contained 10 μg/ml of purified AAA-ATPase in ATPase binding buffer (ATPaseBB: 20 mM HEPES/KOH pH 7.4, 150 mM KCl, 1 mM $MgCl_2$, 1 mM β-mercaptoethanol, 0.1% (v/v) Triton X-100). The concentration of AtCDC48 in T87 cytosol (S150) was quantified by immunoblotting and scanning densitometry using *E. coli* expressed His_6-T7-AtCDC48 as a standard. Therefore, 275 μg of S150 protein containing 1 μg (11.2 pmol) of AtCDC48 was utilized. Purified *E. coli*-expressed GST-PUX1 constructs were added in molar ratios to AtCDC48 of 0.5, 1, 2, and 3 mol and ratios of 1 and 2 for p97 and NSF, respectively. Reactions were incubated on ice for 30 min followed by affinity isolation using glutathione-Sepharose 4B resin. Bound complexes were washed three times with ATPaseBB and processed for SDS-PAGE. AtCDC48 samples were processed for immunoblotting with anti-AtCDC48 antibodies. NSF and p97 protein samples were analyzed by SDS-PAGE followed by staining with Coomassie R-250.

Characterization of the Oligomeric Structure of AtCDC48/PUX1 Complexes—*E. coli*-expressed His_6-AtCDC48, His_6-p97, and GST-free PUX1 were used to examine the effect of GST-free PUX1 on the oligomeric status of these AAA-ATPases. To test the effect of full-length and PUX1-domain fragments on the oligomeric status of AtCDC48 and p97, PUX1-derived proteins were mixed with the AAA-ATPase at molar ratios of 1:3, 1:1, and 3:1 PUX1:AAA-ATPase and incubated in the absence or presence of exogenous nucleotides (1 mM final concentration for ATP, ADP, or AMP-PNP) for 30 min on ice prior to sucrose gradient fractionation. 30 μg of total protein was fractionated on a 5-ml 20–40% (w/w) sucrose gradient (20 mM HEPES/KOH pH 7.4, 150 mM KCl, 1 mM $MgCl_2$, 1 mM β-mercaptoethanol). Gradients were centrifuged at 128,000 × *g* in a SW50.1 rotor (Beckman Coulter, Fullerton, CA) for 18 h at 4 °C. The protein sedimentation standards used included ovalbumin (3.6 S, 43.5 kDa), bovine serum albumin (4.4 S, 66 kDa), and apoferritin (17.7S, 480 kDa). Standards were run on gradients parallel to samples. In addition, the refractive indices for gradient fractions were used to cross-reference peak assignments between gradients. Fractions were collected and analyzed as described (35).

Oligonucleotides Used in This Study—All oligonucleotides used in this study were synthesized by Integrated DNA Technologies (Coralville, IA) (Table I). Uppercase sequences represent those complementary to the *PUX1* (At3g27310) locus. Lowercase nucleotides correspond to sequences added to aid in cloning. Translational stop codon sequences are underlined.

Cloning of PUX1 cDNA, Protein Expression, and Antibody Production—A *PUX1* cDNA was obtained by RT-PCR using primers SB214/SB215 from T87 suspension-cultured cell total RNA prepared as described (40). The amplified product was cloned into pGEM-T easy (Promega) and sequenced using primers SB93 and SB94. An *E. coli* protein expression vector was constructed by subcloning an EcoRI *PUX1* fragment from pGEMT-easy/*PUX1*-cDNA into pGEX4T-3 (Amersham Biosciences). This strategy resulted in the addition of 5 amino acids (DSLVI), encoded by flanking nucleotide sequence derived from the pGEMT-easy vector, into the linker between the GST and the N terminus of the *PUX1*.

pGEX4T-3-PUX1 was expressed in *E. coli* strain BL21(DE3)pLys at 37 °C using 0.5 mM isopropyl-β-D-thiogalactopyranoside (IPTG) for 3 h and affinity-purified using glutathione-Sepharose 4B as described (35). *E. coli*-expressed GST-free PUX1 was generated from GST-PUX1 using a thrombin cleavage capture kit (Novagen). Protein samples were stored as aliquots at −80 °C.

Polyclonal rabbit antibodies were generated against the GST-PUX1 fusion protein at Covance Research Products Inc. (Denver, PA) using standard protocols. Antiserum was cleared of anti-GST antibodies followed by affinity purification of anti-PUX1 antibodies on a DMP-coupled GST-PUX1/glutathione-Sepharose 4B resin as described (35).

Arabidopsis T87 Subcellular Fractionation and PUX1 Purification—Protocols for subcellular and glycerol gradient fractionation of Arabidopsis cytosol were performed as described (35). For co-immunoprecipitation of PUX1 and AtCDC48, affinity-purified anti-PUX1 antibodies were bound and coupled chemically to Protein A-Sepharose beads at a concentration of 0.1 mg/ml using DMP as above. Arabidopsis S150 (100 μg of protein) in MIB was cross-linked chemically using 0.5 mM 3,3′-dithio bis(sulfo-succinimidylpropionate) (DTSSP; fresh stock in dH_2O; Pierce) for 30 min at 4 °C. Reactions were quenched by the addition of Tris-HCl, pH 7.5 (final concentration of 50 mM) followed by a 20-min incubation at 4 °C. PUX1-containing protein complexes were immunoisolated using conjugated anti-PUX1 antibody protein-A-Sepharose (2 μg of antibody per reaction). Isolated protein complexes were washed three times with MIB, solubilized in 2× SDS-PAGE sample buffer supplemented with 100 mM DTT and analyzed by SDS-PAGE and immunoblotting against either AtCDC48 or PUX1. Immunoblot detection was performed using horseradish peroxidase-conjugated secondary

TABLE I
Oligonucleotides used in study

Name	Sequence (5′-3′)	Purpose
SB40	gtcagatctaacttgagg	AtCDC48A sequencing
SB42	catattcattgatcagatcgactctattgcaccg	AtCDC48A sequencing
SB43	cggtgcaatagagtcgatctgatcaatgaatatg	AtCDC48A sequencing
SB58	cattttataataacgctgcggacatctaca	JL202; T-DNA left border
SB62	ggagttcctgacgaaattggacg	AtCDC48A sequencing
SB93	gtaatacgactcactatagggc	T7 promoter; sequencing
SB94	atttaggtgacactatagaatac	SP6 promoter; sequencing
SB149	gagggtacctcaagaatcagtatcactttccccagt	AtCDC48A sequencing
SB214	ATGTTTGTTGATGACCCTTCTC	5′-PUX1 cDNA cloning
SB215	TCACATTTTAAACCACTTAGGC	3′-PUX1 cDNA cloning
SB223	AAGTAAAGAATAACTTGAACCGGGTCTGA	5′-PUX1 T-DNA insertion screen
SB224	CGACACAATAAGATTGCTACTGTGAAGTG	3′-PUX1 T-DNA insertion screen
SB227	cgggatccATGTTTGTTGATGACCCTTCT	5′-PUX1 cDNA, N-terminus clones; BamHI
SB228	ggaattcTCACATTTTAAACCACTTAGGC	3′-PUX1 C-terminal clone; EcoRI
SB371	tcagtatcagcggccgcagtaatccaaaagtagag	3′-His_6-T7-AtCDC48A cloning; NotI
SB405	tggcccggggcgacccatttgctgtccaccagtcatgctagccatgc	3′-primer extension for His_6-T7 cloning; SmaI
SB406	ccacccgggatgcatcatcatcatcatcacagcatggctagcatgac	5′-primer extension for His_6-T7 cloning; SmaI
SB407	ccacccgggatgcatcatcatcatcatcac	His_6-T7 sequencing
SB408	ggttgcagggtgaagagagacgacgga	His_6-T7-AtCDC48A sequencing
SB439	ggaattccatatgcatcatcatcatcatcac	5′-His_6-T7-AtCDC48A cloning; NdeI
SB483	atgtcgactcaAGCTTCTTCTGCTTCC	3′; stop codon before PUX1 UBX; SalI
SB484	aagtcgactcaTGAAAAGTAGACAATG	3′; stop codon after PUX1 UBX; SalI
SB502	gtggatccGCTCGTCGATCAAAGCTCA	5′; PUX1 UBX; BamHI
SB503	agcggatccAACGATCAACCTAAAGATG	5′; PUX1 C-terminal clone; BamHI

antibodies, ECL chemiluminescence detection kit (Amersham Biosciences), and exposure to film (Fuji Photo Film Co. Ltd., Tokyo, Japan).

Cloning and E. coli Protein Expression of His-tagged AtCDC48 and PUX1 Truncation Mutants—A His_6-T7 epitope tag was generated by primer extension using complementary primers SB405 and SB406, and ligated into a SmaI restriction site 74-bp upstream of the endogenous translational start site of AtCDC48A in pPZP211 (41). The cDNA encoding His_6-T7-tagged AtCDC48 was PCR-amplified using primers SB439/SB371, TA-cloned into pGEM-T Easy (Promega) and sequenced using primers SB40, 42, 43, 62, 149, 407, and 408. A NdeI/NotI restriction fragment containing the His_6-T7-*AtCDC48* cDNA was cloned into pET29A for protein expression in *E. coli*. His_6-T7-AtCDC48A protein was expressed in the *ROSETTA* (Novagen) strain of *E. coli* at 28 °C using 100 μM IPTG for 3 h and purified using Ni-NTA (Qiagen) as described (27) with the exception that 2 mM β-mercaptoethanol was used instead of DTT.

GST-PUX1 truncation mutant constructs were generated by PCR amplification of cDNA fragments from pGEX4T-3-*PUX1*. Fragments were cloned into a modified pGEX4T-3 vector with a Tev protease cleavage site (pGEX4T-3-TEV) (42) using either BamHI/SalI or BamHI/EcoRI. The mutants were generated by PCR amplification using the following oligonucleotide sets: (*a*) N terminus (amino acids 1–100; primers SB227 and SB483), (*b*) UBX (amino acids 100–181; primers SB502 and SB484), (*c*) C terminus (amino acids 181–251; primers SB503 and SB228), (*d*) N terminus+UBX (amino acids 1–181; primers SB227 and SB484), and (*e*) UBX+C terminus (amino acids 100–251; primers SB502 and SB228). Proteins were expressed in *ROSETTA E. coli* at 37 °C using 100 μM IPTG induction for 3 h and affinity-purified using glutathione-Sepharose 4B as described above. GST-free forms were generated by TEV protease treatment of glutathione-Sepharose bound GST fusion proteins in TBS pH7.4 overnight at 22 °C at a mass ratio of 1 μg of recombinant His_6-TEV to 20 μg GST-protein. Recombinant His_6-TEV was removed using Ni-NTA agarose, and the GST-free proteins were quantified and stored at −80 °C. The purity of all *E. coli*-expressed proteins was assessed by SDS-PAGE and Coomassie Blue staining.

Kinetic Analysis of AtCDC48 Enzyme Activity—Kinetic analysis was performed with purified His_6-T7-AtCDC48A protein expressed in *E. coli*. 50-μl assays were performed with 0.3 μg (0.067 μM) of His_6-T7-AtCDC48A protein in reaction buffer (20 mM HEPES/NaOH pH 7.4, 5 mM $MgCl_2$, 150 mM NaCl, 1 mM DTT) with the specified ATP concentrations (0.05–0.2 mM) at 22 °C. Colorimetric detection of phosphate product release was performed as described (43) in a 96-well microtiter plate format with absorbance measurements performed on a microplate reader (Bio-Tek, Winooski, VT) equipped with a 660-nm filter. Inhibition studies with purified *E. coli*-expressed GST-free PUX1 (0.048–0.576 μg of PUX1 protein; 0.034–0.402 μM) were performed using 15-min fixed point assays under reaction conditions described above.

Isolation of pux1 T-DNA Insertion Mutants—PCR-based identification of T-DNA insertions in *PUX1* was performed as described (44). Two independent insertion lines were identified in the Alpha population lines present at the Arabidopsis Knock-out Facility (Biotechnology Center, University of Wisconsin, Madison, WI) using gene-specific PCR primers SB223 and SB224 and the T-DNA left border primer JL202 (SB58). DNA sequencing of the PCR-amplified products determined the T-DNA insertion positions within *PUX1*. Heterozygous *pux1* plants were backcrossed to wild-type WS ecotype plants. Mutiplex PCR using primers SB223, 224, and 58 was used to confirm the genotypes of segregating plants.

Plant Growth and Analysis—Surface-sterilized seed were either plated on solidified half-strength Murashige and Skoog (45) (0.5× MS) medium plates (base recipe: 2.15 g/liter MS salts (Invitrogen Life Technologies), 2.6 mM 2-(*N*-morpholino)-ethanesulfonic acid, 0.8% (w/v) Phytagar (Invitrogen Life Technologies), pH to 5.7 with 1 mM KOH) in the presence or absence of sucrose (1 or 3% (w/v)), or imbibed with sterile water and cold-treated (4 °C) in the dark for 3–4 days. Plated seeds were germinated and grown vertically under constant fluorescent lighting at 22 °C for 7 days. Roots length was measured on days 2, 4, and 6 after transfer from 4 to 22 °C. Averages and standard errors were calculated for groups of 10 seedlings per medium per genotype. Consecutive confocal micrograph images of propidium iodide-stained roots from wild-type WS and *pux1* mutant 6-day seedlings were obtained with a Bio-Rad 1024 confocal microscope using a 25× objective lens. 20 frames were averaged for each image. Inverse coloration and composite generation was performed using Adobe Photoshop 6.0 software.

Imbibed seed was sown onto soil (Superfine Germination Mix, Conrad Fafard, Agawam, MA) treated with Adept© (Uniroyal Chemical Company Inc., Middlebury, CT) and grown under fluorescent light illumination cycles of 16 h on and 8 h dark at 22 °C. Plants were fertilized once with diluted Dyna-Gro© Liquid Grow plant food (7-9-5, diluted 3 ml/liter; Dyna-Gro Corp., San Pablo, CA). Total leaf numbers and influorescence lengths were determined. Primary bolt length was measured from the rosette to the apical meristem every other day from the time of bolt emergence to the time that vertical growth ceased.

General Reagents and Antibodies—Molecular biology enzymes were purchased from New England Biolabs (Beverly, MA) or Amersham Biosciences. *E. coli* expression plasmids for mouse p97 and mammalian NSF were provided by H. Meyer (ETH, Zurich, Switzerland) and T. Martin (University of Wisconsin-Madison), respectively. Antibodies against AtSEC12, phosphoglycerokinase (PGK), NSF, and tubulin have been described previously (35, 40). Donkey anti-rabbit, sheep anti-mouse, and rabbit anti-chicken horseradish peroxidase conjugates were purchased from Amersham Biosciences and Jackson ImmunoResearch Laboratories, Inc. (West Grove, PA). All other reagents unless specified were from Sigma and Fisher. Protein assays were performed using a Bradford assay kit (Bio-Rad) and bovine serum albumin as a standard.

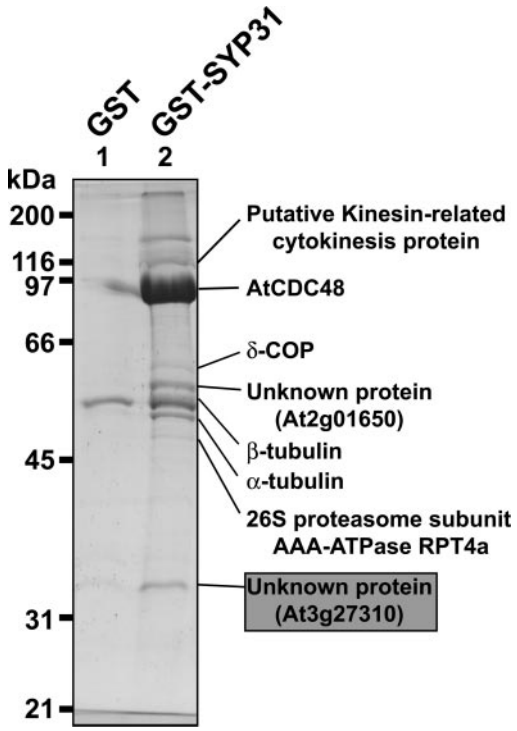

FIG. 1. **Identification of Arabidopsis PUX1.** Coomassie Blue-stained analytical SDS-polyacrylamide gel of immobilized GST or GST-SYP31 affinity-purified cytosolic protein. MALDI-TOF mass spectrometric identification of individual proteins is indicated to the *right* of the respective protein bands.

RESULTS

Tandem SYP31 Affinity Chromatography/MADLI-TOF Mass Spectrometry Identification of PUX1—We have demonstrated previously that the Arabidopsis syntaxin SYP31 and AtCDC48 interact and colocalize at the division plane during cytokinesis (35). Interaction of mammalian p97 with syntaxin 5 is mediated by the soluble protein adapter p47. To identify functional plant homologs of p47 required for SYP31-AtCDC48 interaction, cytosolic protein from Arabidopsis suspension-cultured cells (T87, Ref. 46) was incubated with immobilized GST (control) or GST-SYP31 fusion protein lacking its transmembrane anchor under conditions that support AtCDC48/SYP31 interaction (35). Soluble proteins that bound exclusively to GST-SYP31 were identified by Coomassie Blue staining after SDS-PAGE and processed for MALDI-TOF mass spectrometry. The protein profiles for bound proteins eluted with 250 mM NaCl and the identification of 8 polypeptides that bound to GST-SYP31 are presented in Fig. 1. AtCDC48 and several other characterized proteins were identified including α- and β-tubulin, δ-COP, a component of the Golgi COPI vesicle coat protein complex, and RPT4a, a regulatory AAA-ATPase 19 S-base component of the 26 S proteasome. In addition, three uncharacterized proteins were identified that are encoded by the loci At2g36200, which encodes a kinesin-like family heavy chain, At3g27310 and At2g01650.

Analysis of the deduced primary amino acid sequences for At3g27310 and At2g01650 suggested that these proteins contain single UBX domains. The Arabidopsis genome contains at least 15 *PUX* genes.[2] At3g27310 and At2g01650 have been designated *PUX1* and *PUX2*, respectively. The characterization of PUX1 and its function will be presented here.

A PUX1 cDNA (GenBank™ accession no. AY572781) predicted to encode a protein of 251 amino acids with a predicted molecular mass of 28,484 Da was cloned from total RNA prepared from T87 suspension-cultured cells. The primary amino acid sequence and a schematic for the protein domain structure are presented in Fig. 2, *A* and *B*.

PUX1 is a unique gene in the Arabidopsis genome and putative PUX1 orthologs have been identified in other plants including rice (*Oryza sativa*;*Os*). The alignment of the deduced amino acid sequences of PUX1 and OsPUX1 (GenBank™ accession no. CAE03155), which share 45% sequence identity (61% similarity) over the entire length of the protein is presented in Fig. 2*A*. Further analysis of the plant genome data bases available through The Institute for Genomic Research (TIGR) demonstrated that PUX1-like proteins are likely expressed in other eudicots and monocots, many of which are agriculturally important including grape, tomato, potato, cotton, corn barley, wheat, sorghum, and soybean.[2] MPSS expression profile data from Arabidopsis (mpss.udel.edu/at/java.html) suggested that the *PUX1* gene is expressed ubiquitously *in planta*. Proteins containing regions of similarity and domain organization to full-length PUX1 have also been identified using PSI-BLAST (47) in mouse (GenBank™ accession nos. NP_081153 and NP_937866; 26% identity and 43% similarity), human (GenBank™ accession no. NP_076988; 28% identity and 42% similarity), *Drosophila melanogaster* (GenBank™ accession no. NP_611356; 20% identity and 39% similarity) and *Caenorhabditis briggsae* (GenBank™ accession no. CAE64789; 15% identity and 31% similarity) suggesting that the function of PUX1 may be conserved between plants and animals. In addition, PUX1 homologs were identified in a limited number of fungi including *Eremothecium gossypii* (GenBank™ accession no. NP_984246; 22% identity and 38% similarity), *Aspergillus nidulans* (GenBank™ accession no. EAA60215; 17% identity and 31% similarity), and *S. cerevisiae* (GenBank™ accession no. NP_013783; 17% identity and 31% similarity). No PUX1-like proteins were identified eubacteria.

Because the predicted 28 kDa PUX1 protein was originally identified as a 34 kDa polypeptide by GST-SYP31 affinity chromatography and SDS-PAGE (Fig. 1), the GST-SYP31/PUX1 interaction results were verified by immunoblot analysis. Immunoblot analysis of GST- and GST-SYP31 affinity-purified T87 cytosolic proteins using affinity-purified polyclonal anti-PUX1 antibodies confirmed that the cytosolic 34 kDa polypeptide that bound to GST-SYP31 corresponded to PUX1 (Fig. 3*A*, *lane 3*). In addition to the 34 kDa protein, a 38 kDa polypeptide copurified with $PUX1^{34kDa}$ by SYP31 affinity chromatography and was detected by immunoblotting using anti-PUX1 antibodies (Fig. 3*A*). As shown below, both of these proteins are encoded by *PUX1* (Fig. 7*A*).

PUX1 Is a Soluble Protein That Co-fractionated with Non-hexameric AtCDC48—The subcellular distribution of PUX1 was determined by the differential centrifugation of a T87 cell post-nuclear supernatant (S1). Relative to the fractionation profile of the cytosolic and membrane subcellular markers, phosphoglycerokinase (PGK; S150) (40), and AtSEC12 (endoplasmic reticulum; P150) (48), respectively, PUX1 was detected only in the S150 fraction (Fig. 3*B*). This is in marked contrast to the subcellular distribution of the integral, SYP31 (P150), and peripheral, AtCDC48, membrane-associated proteins (35) (Fig. 3*B*).

In contrast to the mammalian p97 adapter, p47 (21), PUX1 did not co-fractionate with soluble hexameric AtCDC48. This was demonstrated by glycerol gradient velocity sedimentation centrifugation (VSC) fractionation of T87 cytosol (S150) and immunoblotting for AtCDC48 and PUX1 (Fig. 3*C*). As described (35), the majority of cytosolic AtCDC48 was associated with higher order oligomers (Fig. 3*C*, *lanes 15–21*; ≥17.7S). In

[2] D. Rancour and S. Bednarek, unpublished data.

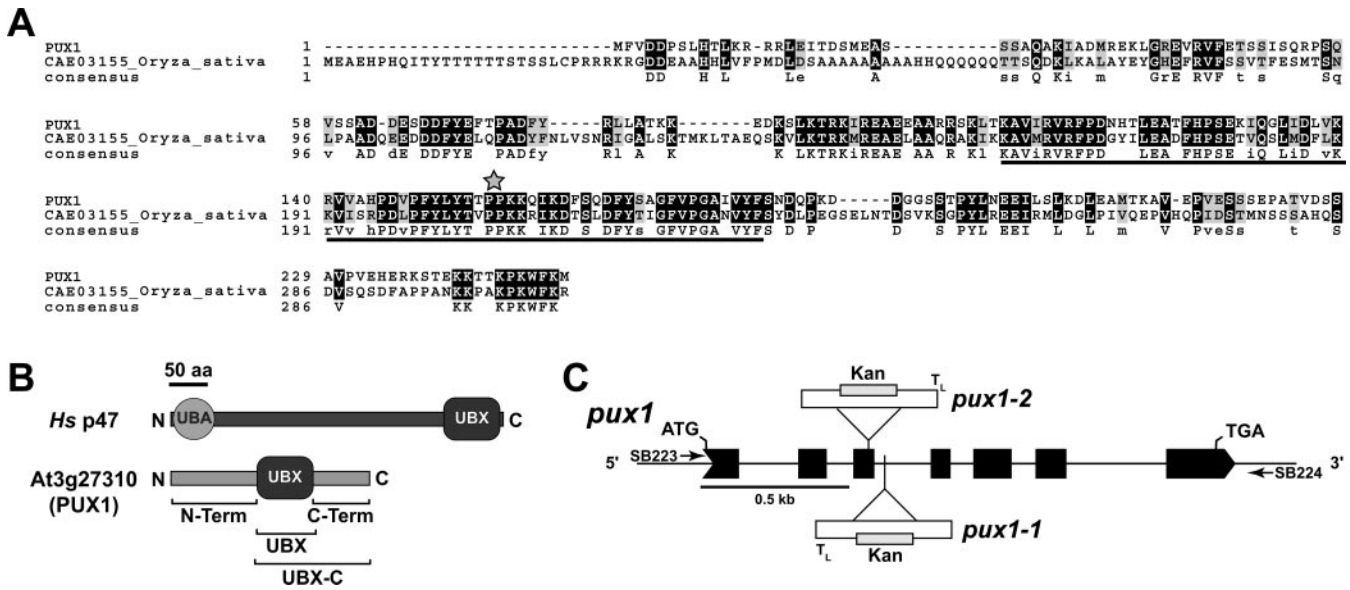

FIG. 2. **PUX1 protein sequence, protein domain and gene organization, and T-DNA insertion sites.** *A*, deduced protein sequence for Arabidopsis PUX1 (*upper sequence*) and its putative *Oryza sativa* ortholog (*lower sequence*). The alignment with a consensus sequence was established using ClustalW (75, 76). Identical amino acids are highlighted with *black*, and similar amino acids are highlighted with *gray*. A *solid bar* underlines the location of amino acids corresponding to the UBX domain. The *star* denotes amino acids of PUX1 that correspond to the FP-motif found in the p47 UBX-domain (see "Discussion"). *B*, protein domain organization of *Homo sapiens* p47 adapter protein and Arabidopsis PUX1 (At3g27310). The protein domains presented include UBX, ubiquitin-like protein fold (InterPro domain: IPR001012), and the UBA, ubiquitin-associated domain (InterPro domain: IPR000449). The *scale bar* corresponds to 50 amino acids. The brackets under PUX1 represent the subdomains of PUX1 that were used for generation of truncation protein mutants used in this study. *C*, intron/exon organization of *PUX1* and the positions of T-DNA insertion sites in *pux1* lines. *Broad bars* represent exons and *narrow lines* represent introns. Translational start and stop codons are indicated. Exons and introns are drawn to scale (*bar* = 500 bp). T-DNA inset is not drawn to scale. *npt*, neomycin phosphotransferase T-DNA selection marker gene; T_L, T-DNA left border.

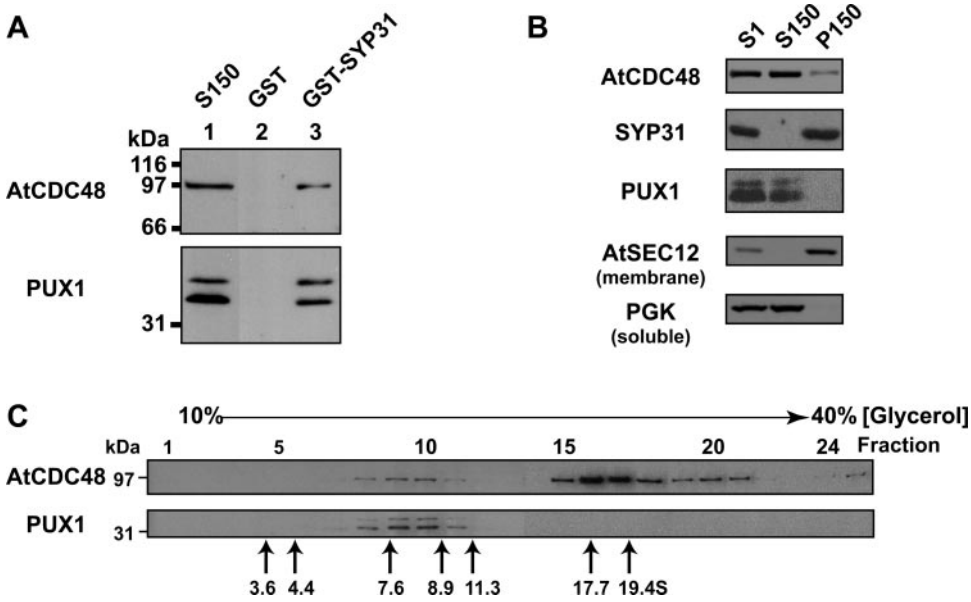

FIG. 3. **PUX1 is a soluble protein that co-fractionated with non-hexameric AtCDC48.** *A*, immunoblot verification that PUX1 interacted with GST-SYP31. T87 cytosol (20 μg of S150 in *lane 1*) was subjected to affinity chromatography using immobilized GST (*lane 2*) and GST-SYP31 (*lane 3*), and eluted proteins were analyzed by immunoblotting with anti-AtCDC48 (*upper panel*) and anti-PUX1 (*lower panel*) antibodies. *B*, PUX1 is a soluble protein as determined by subcellular fractionation. T87 postnuclear supernatant (*S1*), S150 and P150 (20 μg per lane) were analyzed by SDS-PAGE and immunoblotting using antibodies directed against AtCDC48, SYP31, PUX1, and the membrane and cytosolic protein markers AtSEC12 and PGK, respectively. *C*, PUX1 co-fractionated with non-hexameric cytosolic AtCDC48. 4×10^6 equivalents of T87 protoplast S150 was fractionated by continuous glycerol gradient (10–40% (v/v)) sedimentation and individual fractions were analyzed by SDS-PAGE and immunoblot for either AtCDC48 (*upper panel*) or PUX1 (*lower panel*). The gradient sedimentation standards are indicated at the *bottom* and are in Svedberg (S) units.

addition, a small but reproducible non-hexamer fraction (*lanes 7–11*; ~8 S) of AtCDC48 was detected, and PUX1 co-fractionated exclusively with this latter AtCDC48 pool.

PUX1 Interacts with the AtCDC48/p97 Class of AAA-ATPases—To address whether AtCDC48 and PUX1 interact *in vivo*, we performed immunoprecipitation experiments using anti-PUX1 antibodies (Fig. 4*A*) in the presence and absence of the thiol-reductant cleavable chemical cross-linking reagent DTSSP. As shown in Fig. 4*A*, reproducible co-immunoprecipitation of AtCDC48 via PUX1 was dependent upon pretreatment of cytosolic fractions with DTSSP (Fig. 4*A*, *lane 2*) and was strictly dependent upon the presence of PUX1 antibodies (Fig. 4*A*, *lane 3*).

PUX1 Binds Directly to AtCDC48—To test whether PUX1

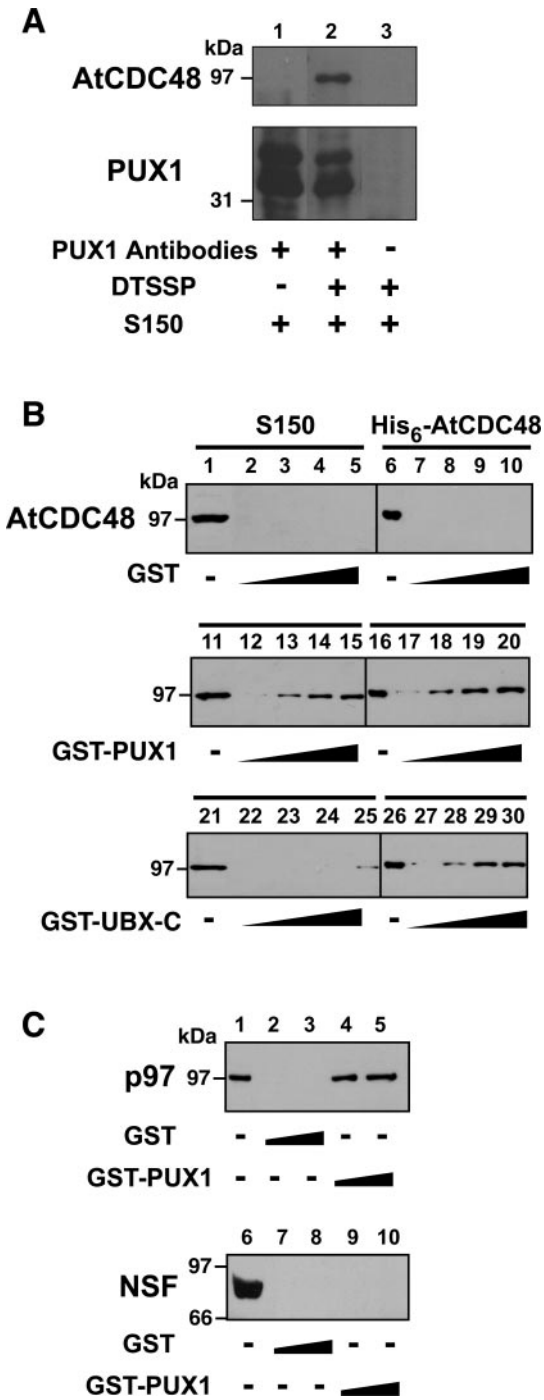

FIG. 4. **PUX1 interacted specifically with the CDC48/p97 class of AAA-ATPases.** *A*, co-immunoprecipitation of PUX1 and AtCDC48 from T87 cytosol. T87 S150 was mock-treated (*lane 1*) or treated with cross-linker (DTSSP, *lanes 2* and *3*) and subjected to immunoprecipitation using either anti-PUX1 antibodies coupled to protein A-Sepharose (*lanes 1* and *2*) or protein A-Sepharose alone (*lane 3*). Isolated protein complexes were analyzed by SDS-PAGE and immunoblotting with anti-AtCDC48 (*upper panel*) and anti-PUX1 (*lower panel*) antibodies. *B*, interaction of PUX1 with AtCDC48 requires the UBX and C terminus of PUX1. Cytosolic AtCDC48 and purified His_6-T7-AtCDC48 binding assays were performed with GST control (*upper panel*), full-length GST-PUX1 (*middle panel*), and the PUX1 truncation mutant fusion protein, GST-UBX-C (*lower panel*). The source of AtCDC48 in the binding reactions (11.2 pmol per reaction) was from either a T87 cytosolic protein fraction (S150; *lanes 1–5*, *11–15*, and *21–25*) or purified *E. coli* expressed AtCDC48 (His_6-T7-AtCDC48; *lanes 6–10*, *16–20*, and *26–30*). GST and GST-PUX1 fusion proteins were added at molar ratios of 0.5 (*lanes 2*, *7*, *12*, *17*, *22*, and *27*), 1 (*lanes 3*, *8*, *13*, *18*, *23*, and *28*), 2 (*lanes 4*, *8*, *14*, *19*, *24*, and *29*), and 3 mol (*lanes 5*, *10*, *15*, *20*, *25*, and *30*) per mol of AtCDC48. AtCDC48 loading controls are given in *lanes 1*, *6*, *11*, *16*, *21*, and *26*. *C*, PUX1 interacts with mammalian p97 but not NSF. Coomassie Blue-stained *in vitro* binding assay results of either mammalian p97 (*upper panel*) or mammalian NSF (*lower panel*). Interactions with GST (*lanes 2*, *3*, *7*, and *8*) or GST-PUX1 (*lanes 4*, *5*, *9*, and *10*) were tested. 11.2 pmol of p97 or NSF were incubated in the presence of GST fusion proteins added at molar ratios of 1 (*lanes 2*, *4*, *7*, and *9*) and 2 mol (*lanes 3*, *5*, *8*, and *10*) per mol of AAA-ATPase. Loading controls are presented in *lanes 1* and *6* for p97 and NSF, respectively.

directly binds to AtCDC48, an *E. coli*-expressed His_6-T7 N-terminal-tagged AtCDC48 was generated. Purified His_6-T7-AtCDC48 demonstrated ATP hydrolytic activity that was dependent on time, ATP concentration (Fig. 5*A*), and enzyme concentration.[2] The enzyme exhibited a K_m of 40.5 μM and a V_{max} of 3.47 μM P_i min^{-1} μg^{-1} at 22 °C. These values represent an 8-fold decrease in K_m and a V_{max} 30% of that reported for mammalian p97 (49). Feiler *et al.* (50) had demonstrated that AtCDC48 could functionally replace yeast CDC48 *in vivo*. Similarly, His_6-T7-AtCDC48 fully rescued the growth of the yeast *cdc48–1* temperature-sensitive mutant at 37 °C. In addition, His_6-T7-AtCDC48 was targeted to the division plane in transgenic tobacco cells confirming that the tagged protein was functional *in vivo*.[3]

As shown in Fig. 4*B*, GST-PUX1 precipitated cytosolic and purified AtCDC48. GST did not bind AtCDC48 (Fig. 4*B*, *top panel*) even at the maximal molar ratio of 1 mol of AtCDC48/3 mol of GST. In contrast, full-length GST-PUX1 was able to bind to equivalent amounts of either cytosolic AtCDC48 (S150) or His_6-T7-AtCDC4 (Fig. 4*B*, *middle panel*). In addition, GST-free PUX1 inhibits the ATPase activity of His_6-T7-AtCDC48 (Fig. 5*B*). Kinetic analysis of PUX1 inhibition suggested that PUX1 was a noncompetitive inhibitor of AtCDC48 ATPase activity. With the exception of AtCDC48, no additional cytosolic proteins were observed to bind to GST-PUX1 by SDS-PAGE and Coomassie Blue staining.[2]

To determine the domain requirements for PUX1 interaction with AtCDC48, we made several PUX1 truncation mutants (Fig. 2*B*) and tested their ability to bind AtCDC48 *in vitro*. The PUX1 UBX-C truncation mutant (UBX-C; amino acids 100–251; *schematic 2B*) interacted with His_6-T7-AtCDC48 with the same efficiency as full-length PUX1 (Fig. 4*B*, *lower panel*). Interestingly, the efficiency of binding of the UBX-C PUX1 mutant with cytosolic AtCDC48 was reduced relative to full-length PUX1 (compare Fig. 4*B*, *lanes 25* and *30*). As shown in Figs. 4*B* and 6*B* (*lane 3*), PUX1/AtCDC48 binding was not dependent on the N terminus of PUX1 (*N-term*; amino acids 1–99, *schematic 2B*). In addition, the PUX1 UBX, and C terminus mutants (Fig. 2*B*) did not have detectable interaction with AtCDC48. Binding of PUX1 and UBX-C to AtCDC48 did not show a requirement for nucleotide.[3]

Arabidopsis PUX1 was found also to bind to the mammalian ortholog of AtCDC48, p97, but not to another hexameric AAA-ATPase, NSF (Fig. 4*C*). These results indicate that the activity of PUX1 is conserved but limited to the p97/CDC48 subfamily of type II AAA-ATPases.

PUX1 Facilitated Disassembly of Hexameric CDC48/p97—Data presented above demonstrated that PUX1 physically interacted with AtCDC48 *in vivo* and *in vitro*, and that endogenous PUX1 was associated with non-hexameric cytosolic AtCDC48. Thus, we tested whether PUX1 modulated the oligomeric structure of AtCDC48. VSC analysis of purified GST-free PUX1 alone was consistent with PUX1 being a monomer (~30 kDa) (Fig. 6*A*), whereas the majority of His_6-T7-AtCDC48 sedimented at ~17.7 S (Fig. 6*B*); smaller than observed for cytosolic AtCDC48 (Fig. 3*C*). A minor peak of non-hexameric

[3] S. Park and S. Bednarek, unpublished data.

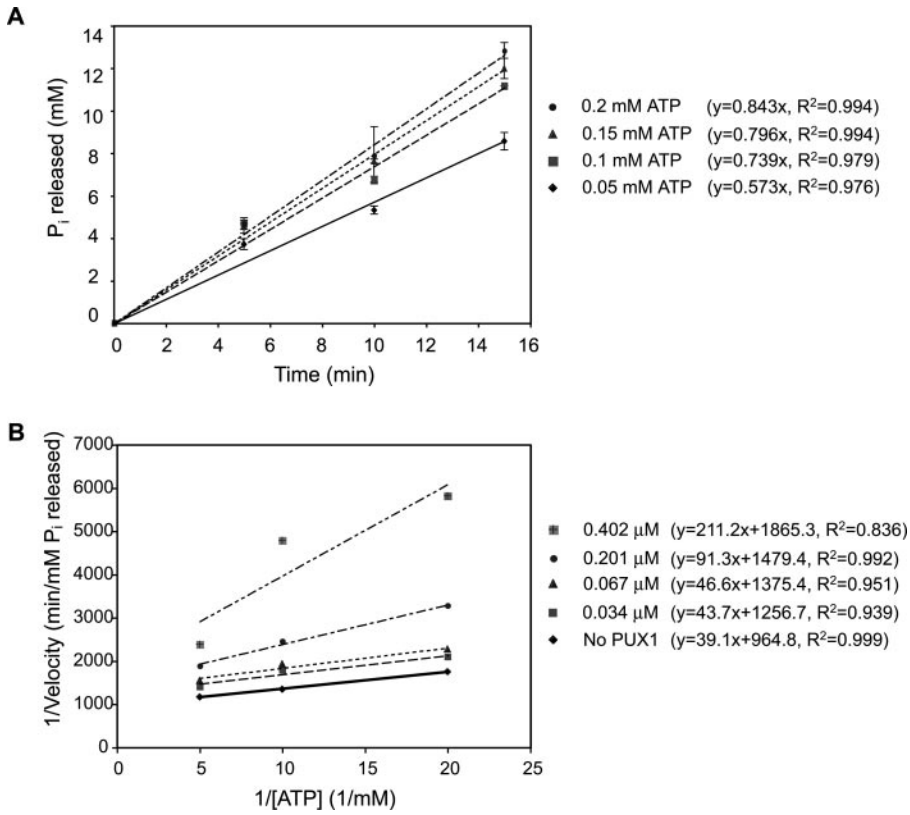

FIG. 5. **PUX1 inhibited the ATP hydroysis activity of AtCDC48.** *A*, kinetic analysis of His_6-T7-AtCDC48 activity. 50-μl assays were performed with 0.3 μg (0.067 μM) of purified His_6-T7-AtCDC48A protein in reaction buffer with specified ATP concentrations (0.05–0.2 mM) at 22 °C for the indicated time. Ammonium molybdate/malachite green colorimetric detection of phosphate product release was performed. Values represent the mean ± S.D. of triplicate determinations. Linear regressions and coefficients of determination (R^2 values) are presented for each data set. *B*, PUX1 is a noncompetitive inhibitor of AtCDC48. Double reciprocal plots for the activity of His_6-T7-AtCDC48 in the absence (*No PUX1*) or presence of PUX1 (0.034–0.402 μM) are presented. Inhibition studies with purified *E. coli*-expressed GST-free PUX1 (0.048–0.576 μg of PUX1 protein) were performed using 15-min fixed point assays under reaction conditions used in *panel A*. Values represent the mean of triplicate determinations. Linear regressions and coefficients of determination (R^2 values) are presented for each data set.

His_6-T7-AtCDC48A (≥4.4 S) was also frequently detected (Fig. 6*B*, *lanes 6–8*, and Fig. 7*A*, *lanes 6–8*). Several significant changes occurred to the sedimentation profiles of PUX1 and His_6-T7-AtCDC48 when they were incubated together at a molar ratio of 3:1 in the absence of exogenous nucleotide and fractionated by VSC (Fig. 5*C*). First, the migration of PUX1 into the gradient increased in the presence of His_6-T7-AtCDC48 (Fig. 6*C*, *upper panel*). Conversely, the sedimentation of His_6-T7-AtCDC48 was retarded in the presence of PUX1 such that it fractionated predominantly at >4.4 S (Fig. 6*C*, *lower panel*, migration peak at fractions 8 and 9) with little hexamer remaining (fraction 15). The sedimentation peak value for *in vitro* disassembled His_6-T7-AtCDC48 was smaller than that observed for non-hexameric AtCDC48 *in vivo* (Fig. 3*C*, *fractions 8–11*). These results suggest that PUX1 facilitates the disassembly of hexameric His_6-T7-AtCDC48. The efficiency of His_6-T7-AtCDC48 disassembly was proportional to the molar ratio of PUX1:His_6-T7-AtCDC48 used in the assay. The disassembly of hexameric His_6-T7-AtCDC48 occurred even in the presence of exogenous nucleotide substrate (ATP), product (ADP), or a non-hydrolyzable analog (AMP-PNP) (Fig. 6*D*). Similar to AtCDC48, we found that PUX1 mediated the disassembly of hexameric mouse p97.[3]

As described above, the primary AtCDC48 interaction determinants of PUX1 were contained within the PUX1 UBX-C-terminal fragment (Fig. 4*B*). To test whether UBX-C was sufficient to facilitate the disassembly of the AtCDC48 hexamer, GST-free UBX-C PUX1 was incubated with His_6-T7-AtCDC48 at a molar ratio of 3:1, fractionated by VSC and analyzed by immunoblotting with anti-AtCDC48 antibodies (Fig. 7*A*). In contrast to full-length PUX1 (Fig. 6*C*), the UBX-C and N-terminal fragments of PUX1 did not promote the disassembly of the AtCDC48 complex independently (Fig. 7*A*; compare with Fig. 6*B*). However, when the UBX-C and N-terminal domains were added *in trans*, significant, albeit not equivalent to full-length PUX1 (Fig. 6*C*) levels of non-hexameric AtCDC48 were observed (Fig. 7*A*, *bottom panel*).

Oligomerization of the UBX-C and N-terminal domains prior to their interaction with AtCDC48 may facilitate the *in trans* disassembly of hexameric AtCDC48. Alternatively, binding of the PUX1 UBX-C domain to AtCDC48 could permit subsequently the binding of the PUX1 N terminus thereby promoting the disassembly of the core hexamer. To test these models, we examined if a GST-N-terminal-PUX1 fusion protein interacted *in vitro* with the UBX-C domain in the presence or absence of His_6-T7-AtCDC48 (Fig. 7*B*). As shown above (Fig. 4*B*), GST-UBX-C interacts with His_6-T7-AtCDC48; however, the GST-tagged N terminus of PUX1 did not interact directly with His_6-T7-AtCDC48 (Fig. 7*B*, *lane 3*). Likewise, limited interaction between the UBX-C region and N terminus of PUX1 was observed (Fig. 7*B*, *lane 1*). Binding of the PUX1 N terminus with His_6-T7-AtCDC48, however, was promoted by the presence of the PUX1 UBX-C domain (Fig. 7*B*, *lane 2*).

pux1 Mutant Plants Exhibited Accelerated Growth Rates—To examine the *in vivo* function of PUX1, we identified two independent *pux1*::T-DNA insertion lines, *pux1–1* and *pux1–2*. The T-DNA insertion sites (Fig. 2*C*) were verified by DNA sequencing of PCR-amplified products using *PUX1* gene-specific (SB223 and SB224) and T-DNA left border (SB58) primers as indicated. *pux1-1* and *pux1-2* (WS ecotype) contain T-DNA insertions within the third intron and exon, respectively, with both alleles displaying identical phenotypes. PCR genotype analysis of the progeny from self-fertilized heterozygous *pux1-1* and *pux1-2* plants demonstrated that the T-DNA mutations behave recessively.

Immunoblot analysis (Fig. 8*A*) of total Arabidopsis protein extracts from homozygous *pux1* and wild-type WS ecotype seedlings and T87 cytosolic protein extract demonstrated that *pux1-1* and *pux1-2* are complete loss-of-function mutants. Disruption of *PUX1* resulted in the loss of the protein doublet (34 kDa and 38 kDa) as detected by immunoblotting with affinity-purified PUX1 antibodies demonstrating that both polypeptides are derived from the same gene (Figs. 3*A* and 8*A*, *upper panel*). Loss of PUX1 did not affect AtCDC48A protein levels

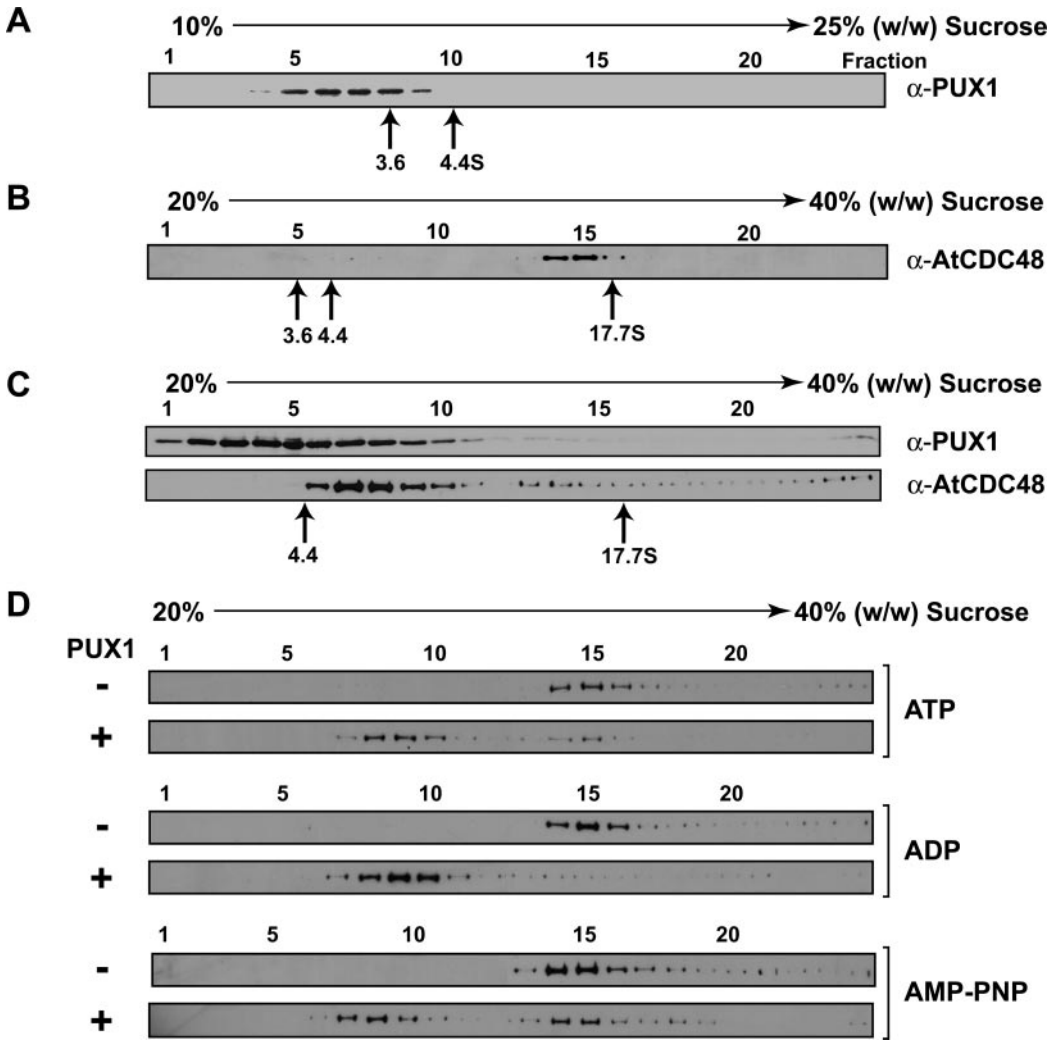

FIG. 6. **PUX1 promoted the disassembly of AtCDC48 hexamers.** *A*, PUX1 fractionates as a monomer. GST-free *E. coli* expressed PUX1 protein (20 μg) was fractionated by sucrose gradient (10–25% (w/w)) velocity sedimentation. *B*, active *E. coli* expressed AtCDC48 fractionates as a hexamer. His_6-T7-AtCDC48 protein (30 μg) was fractionated by sucrose gradient (20–40% (w/w)) velocity sedimentation. *C*, full-length PUX1 promotes the disassembly of hexameric AtCDC48 *in vitro*. *E. coli*-expressed GST-free PUX1 (8.9 μg) and His_6-T7-AtCDC48 (26.8 μg) were mixed, incubated 30 min on ice in the absence of exogenous nucleotide and fractionated by sucrose gradient (20–40% (w/w)) velocity sedimentation. Fractions were analyzed by immunoblotting using anti-PUX1 (*upper panel*) or anti-AtCDC48 (*lower panel*) antibodies. The migration of sedimentation marker proteins ovalbumin (3.6 S, 43.5 kDa), bovine serum albumin (4.4 S, 66 kDa) and/or apoferritin (17.7 S, 480 kDa) is indicated. *D*, PUX1 promotes the disassembly of hexameric AtCDC48 regardless of exogenous nucleotides. His_6-T7-AtCDC48 (26.8 μg) was incubated 30 min on ice with the indicated exogenous nucleotide (1 mM ATP, ADP or AMP-PNP) in the absence (−) or presence (+) of *E. coli*-expressed GST-free PUX1 (8.9 μg) and fractionated by sucrose gradient (20–40% (w/w)) sedimentation. Fractions were analyzed by immunoblotting using anti-AtCDC48 antibodies. Protein peak migrations were identical between gradients as determined by the refractive indices of the gradient fractions.

(Fig. 8*A*, *middle panel*). The 38 kDa PUX1 polypeptide from WS and T87 cells co-migrated with *E. coli* expressed GST-free PUX1.[2] The nature of the molecular mass difference between the two PUX1 isoforms remains to be determined.

Although homozygous *pux1-1* and *pux1-2* displayed no gross morphological abnormalities, the rate at which *pux1* lines grow and reach developmental maturity is accelerated relative to wild type. When grown on nutrient agar medium in the absence of sucrose, the growth of *pux1* roots was ~5-fold faster that wild-type seedlings (Fig. 8*B*). Addition of 1 and 3% (w/v) sucrose to the growth medium increased of the rate of wild-type root elongation almost to *pux1* levels, whereas, exogenous sucrose had only minimal effect on *pux1* mutant root growth rates.

To understand the basis for the increased growth of the roots, confocal microscopic imaging of propidium iodide-stained wild-type WS and homozygous *pux1* 6-day old seedling roots was performed (Fig. 8*C*). The overall cell layer morphology of the roots was the same between wild-type and mutant plants. A striking difference was observed along the root-shoot axis upon alignment of the root quiescent centers (Fig. 8*C*, see *arrows*). Mutant roots appear to have more cells in the division zone, and these cells are more elongated when compared with wild-type WS roots.

Analysis of *pux1* aerial organ growth showed that both *pux1* and wild-type plants flowered with rosettes of similar diameter containing the same number of leaves regardless of day length (*e.g.* leaves for plants grown under long days: 9.6 ± 0.5 for WS, 8.6 ± 0.5 for *pux1-1*, and 9.2 ± 1.1 for *pux1-2*). On the transition to flowering, it was observed that primary inflorescence growth was enhanced in *pux1* (Fig. 8*D*). The initial rates of bolt lengthening were accelerated in *pux1* mutants but overall final height was not altered. These results indicated that the loss of PUX1 does not change major plant developmental programs but merely accelerates them, suggesting a positive role for AtCDC48 in plant growth and that PUX1 functions as a regulator of AtCDC48 function *in vivo*.

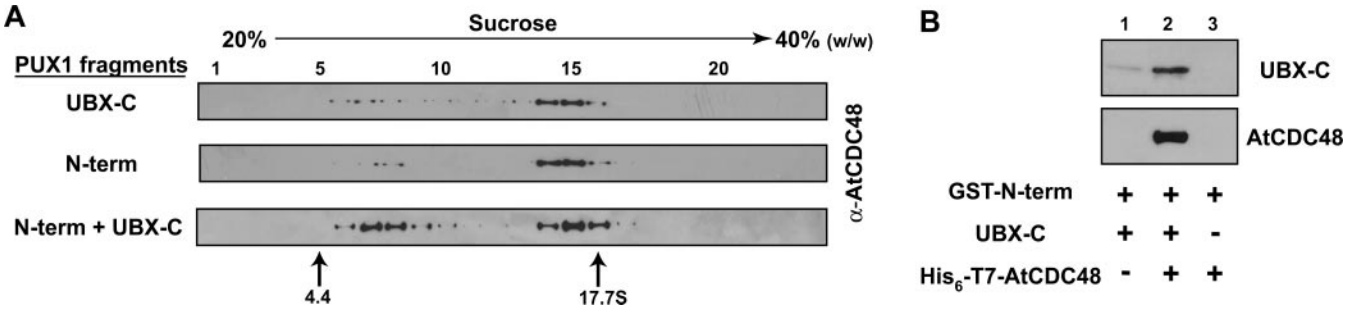

FIG. 7. **PUX1 required both the UBX-C terminus and the N terminus for AtCDC48 disassembly.** *A*, *E. coli*-expressed PUX1 fragments (as indicated to *left* of blot panels) and His_6-T7-AtCDC48 were mixed, incubated 30 min on ice, and fractionated by sucrose gradient (20–40% (w/w)) sedimentation. Fractions were analyzed by immunoblotting for AtCDC48. The migration of sedimentation markers is indicated. *B*, binding of the PUX1 N terminus to AtCDC48 is dependent on the UBX-C. *In vitro* binding assays were performed using GST-PUX1-N terminus as bait. Incubations in the presence of the PUX1 UBX-C-terminal fragment (*lanes 1* and *2*) or His_6-T7-AtCDC48 (*lanes 2* and *3*) were assessed. Bound protein was analyzed by SDS-PAGE and immunoblotting for either PUX1 UBX-C (using anti-PUX1 antibodies; *upper panel*) or AtCDC48 (*lower panel*).

DISCUSSION

Our studies have identified a plant UBX-containing protein, PUX1, which modulates the structure and activity of AtCDC48. AtCDC48 is a member of the p97/CDC48 subclass of conserved type II hexameric AAA-ATPase that functions as a molecular chaperone in numerous diverse cellular activities. Like other AAA ATPases, it is thought that nucleotide-dependent conformational changes in the hexameric p97/CDC48 complex are transmitted mechanically to bound substrates in order to mediate their assembly, disassembly or membrane extraction (4).

The functional oligomeric structure of p97/CDC48 AAA ATPases has been demonstrated by biochemical and structural studies to be a hexamer (11, 35, 51–61). However, small but reproducible quantities of non-hexameric-associated p97/CDC48 have been observed in various organisms (14, 35, 62). The hexameric structure of p97/CDC48 is likely to be an intrinsic property of the ATPases as urea-dissociated p97 subunits can self-reassemble (63). Furthermore, recent evidence showing that epitope-tagged wild-type and ATPase-defective mutant subunits can be incorporated into pre-formed p97/CDC48 hexamers suggests that the oligomeric structure of the chaperone is dynamic *in vivo* (55, 64). The molecular mechanism by which subunit exchange occurs is unknown. To our knowledge, no reports have been made regarding the rate and mechanism of turnover for the p97/CDC48 oligomeric complexes. Here we provide the first evidence that suggests the quaternary structure of the p97/CDC48 family of AAA-ATPases is itself subjected to control and that this control has biological significance. *In vitro* assays have demonstrated that PUX1 promotes the disassembly of hexameric AtCDC48. Consistent with this we have shown by subcellular fractionation that PUX1 co-fractionates and physically associates with soluble non-hexameric AtCDC48.

Data base analysis has shown that PUX1 orthologs exist throughout the plant kingdom and that functional homologs may also be expressed in animals and fungi. Indeed, we have shown that PUX1 interacts and promotes the disassembly of the hexameric mouse p97. The putative animal homologs of PUX1 can be distinguished from other UBX-containing proteins by the presence of a PUX1-like module that shares amino acid similarity to full-length PUX1 including conserved N- and C-terminal regions flanking a centrally located UBX domain. Interestingly, putative PUX1 homologs have been identified in only a limited number of unicellular organisms.

A recurring feature, with regard to the binding to its various effector proteins, is p97/CDC48 ATPase interaction with ubiquitin and ubiquitin-related protein fold domains (22, 26, 28, 30, 32, 61, 64–68). Targeting of the ATPase activity of p97/CDC48 to its various cellular substrates is dependent on specific protein cofactors/adapters (27). These adapters either recruit p97/CDC48 to mono- or poly-ubiquitinated substrates (67) or the adapters themselves contain an ubiquitin-related protein domain (21, 22, 30, 32, 61, 69). Several recent studies, including data presented here, indicate that UBX domains may serve as a general interaction domain for p97/CDC48 (32, 33, 61). The Arabidopsis genome is predicted to encode 15 PUX proteins, and our current working hypothesis is that this protein family may function as specific regulators of p97/CDC48.

Based upon crystallographic analysis, Dreveny *et al.* (61) have proposed that a FP-containing loop between the p47 UBX domain S3 and S4 β-strands is required for interaction with the N-terminal domain of p97/CDC48. In contrast to p47, however, the FP-loop is not conserved in the PUX1 UBX domain (Fig. 2*A*, *star*) where PUX1 has a second proline in place of the phenylalanine. Further work is therefore necessary to define the structural feature(s) contained within the PUX1 UBX-C-terminal fragment that are sufficient for its interaction with AtCDC48 and mouse p97. Similar to p47 (22), we have shown that PUX1 contains a second binding site for AtCDC48 in the N-terminal (amino acids 1–100) fragment. However, we have shown that binding of the PUX1 N terminus to AtCDC48 is facilitated *in trans* by the UBX-C-terminal (amino acids 100–251) domain. Perhaps binding of the UBX-C domain to AtCDC48 causes a conformational change that allows the PUX1 N terminus to bind. Alternatively, AtCDC48 may stabilize weak intramolecular interactions between the PUX1 N terminus and UBX-C domain. Nevertheless, the end result of PUX1 N terminus binding is the disassembly and inactivation of the AtCDC48 oligomer. Experiments to determine if AtCDC48 undergoes intermediate conformational changes (prior to disassembly) upon UBX-C binding and the identification of a cognate binding site(s) on AtCDC48 (*i.e.* the AtCDC48 N-terminal, D1 and/or D2 domains) are in progress.

PUX1 and PUX2 were identified through *in vitro* binding assays under conditions that supported the ATP-dependent interaction of AtCDC48 with the Arabidopsis ortholog of mammalian syntaxin 5, SYP31 (35). PUX1 and the putative Arabidopsis homologs of mammalian p47, PUX3, and PUX4 (which share 34 and 36% identity and 53 and 52% amino acid similarity, respectively, with the human protein), bind AtCDC48 *in vitro* but do not interact with SYP31.[2] Rather, PUX2 functions as the Arabidopsis adapter for interaction between AtCDC48 and SYP31.[4] The role, if any, for PUX1 in AtCDC48/SYP31 interaction remains to be determined. With the exception of AtCDC48 no other soluble proteins were found to interact with

[4] D. Rancour and S. Bednarek, manuscript in preparation.

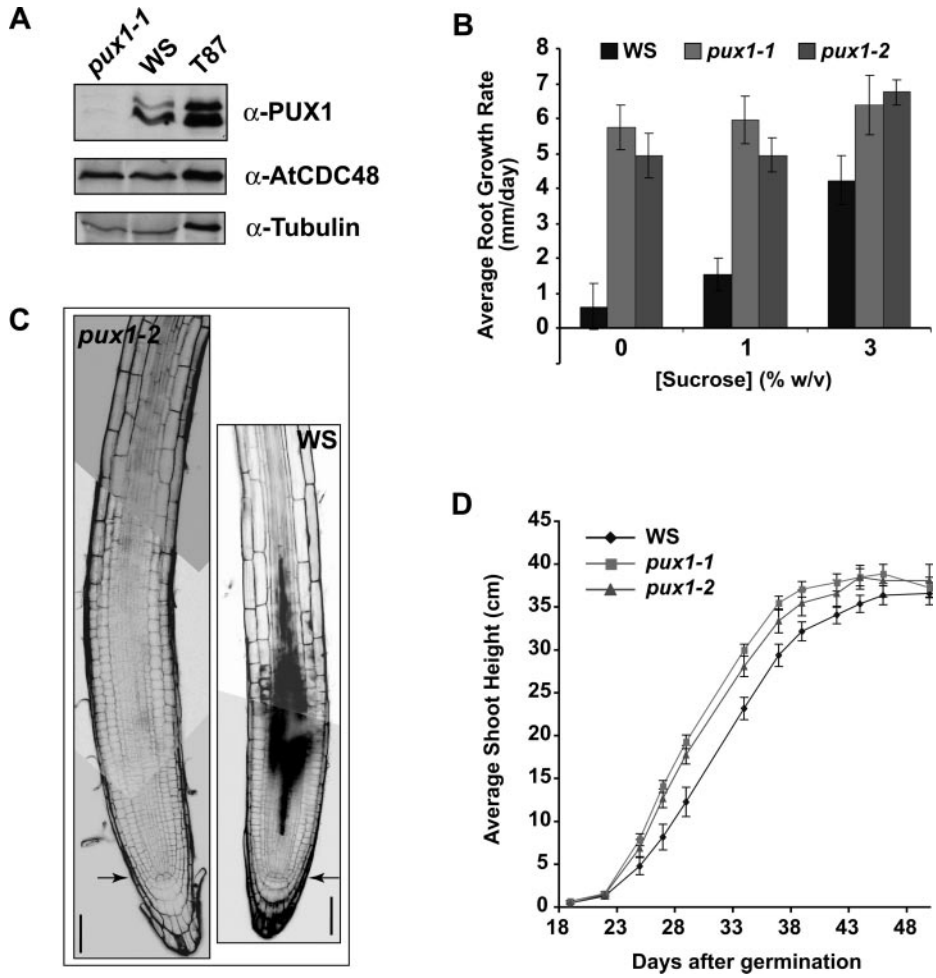

FIG. 8. ***pux1* mutant plants displayed accelerated growth.** *A*, *pux1* mutant plants do not express PUX1 protein. Immunoblot analysis of *pux1–1*, WS (wild-type) and T87 protein extracts. Protein extracts were separated by SDS-PAGE and immunoblotted for PUX1 (*upper panel*), AtCDC48 (*middle panel*), and α-tubulin as a protein loading control (*lower panel*). *B*, *pux1* mutants showed accelerated root growth rates. Cold-treated (3 days, 4 °C, in dark) WS and homozygous *pux1-1* and *pux1-2* seeds were germinated and grown on vertical solid medium ± the indicated sucrose concentration at 22 °C under continuous light. Seedling root growth was monitored from days 2 to 6 after transfer from 4 °C to 22 °C. The data represent a minimum sample size of 10 plants per genotype and condition. The standard deviation is presented for each group. *C*, confocal micrograph composites of WS (wild-type) and *pux1–2* root tips. Roots from 6-day seedlings grown on vertical sucrose-free solid medium at 22 °C under continuous light were stained with propidium iodide and confocal images were taken. Vertical alignment of root images was made relative to the root quiescent centers (see *horizontal arrows*). *Scale bars*, 50 μm. *D*, influorescence elongation was accelerated in *pux1* mutant plants. Primary bolt height was measured from the rosette to the apical meristem from the time of bolt emergence to the time that vertical growth ceased. The data presented are for plants grown under long day conditions (16 h light/8 h dark) at 22 °C. The sample size for each group was 14 WS, 16 *pux1-1*, and 12 *pux1-2*. The standard error is given for each point.

PUX1 suggesting that its function is limited to AtCDC48.

Our hypothesis is that PUX1-mediated disassembly regulates the overall cellular activity of AtCDC48. Previous studies have shown that the chaperone activity of p97/CDC48 is required for a variety of biochemical processes including membrane fusion and proteolysis. Not surprisingly, mutations in p97/CDC48 that affect its activity and/or localization, cause defects in cell cycle progression and cell growth (55, 70, 71). In Arabidopsis, *in situ* hybridization experiments showed that AtCDC48 is highly expressed in dividing and expanding cells (47). Consistent with these observations, we show that loss of a negative regulator of AtCDC48 subunit oligomerization and ATPase activity leads to enhanced root and shoot growth in *pux1* mutants. The relative abundance of AtCDC48 (~1% total T87 protein of which ~85% is soluble, Ref. 35) *versus* PUX1 (~0.029% of soluble T87 protein) and the small amount of AtCDC48-associated PUX1 (Fig. 3*C*) suggests that PUX1-mediated regulation of AtCDC48 activity maybe highly potent during various stages of plant growth and development. One prediction from this model is that increased levels of PUX1 would reduce plant growth. However, no defects in plant growth and development were observed in transgenic T_2 Arabidopsis plant lines that overexpress PUX1. One explanation for this is that the level of AtCDC48 was elevated in the *PUX1* overexpressing lines thereby compensating for the increased amount of PUX1 protein.[2]

Plant growth and development are controlled by the integration of regulated cell division and cell expansion (72). Since plant cells are fixed in their relation to neighboring cells, the balance of division and expansion are needed to control the growth and development of plant structures. Kinematic analysis has shown that Arabidopsis root growth is primarily dominated by the rate of cell division (73). Plant cell division is controlled by various intrinsic and extrinsic signals, including sugar levels that have recently been shown to regulate cell cycle progression in plants by controlling the expression of CycD cyclins (74). Interestingly, the growth rate of wild-type (WS ecotype) roots increased to approximately *pux1* mutant levels in the presence of exogenous sucrose suggesting that loss of a negative regulator of AtCDC48, PUX1, stimulated cell division rates. In addition, cell expansion, which is highly dependent on membrane trafficking and fusion, maybe elevated in the *pux1* mutants due to an increase in the level of active AtCDC48. Consistent with both models, confocal microscopic analysis of the *pux1* mutants suggests that both division and expansion are elevated in *pux1* plants (Fig. 8*C*). Kinematic analysis of *pux1* plants will need to be performed to assess whether the growth rate increases are due to more cell division and/or cell expansion.

Acknowledgments—We thank Dr. Amy Harms for assisting with the mass spectroscopic identification of PUX1, Drs. Graham Warren and Hemmo Meyer for providing the His_6-p97 expression construct, Brent Svac for the analysis of *pux1* plants, and Dr. Judith Kimble for the use of her confocal microscope. We also would like to thank members of our laboratory for discussion and critical reading of the manuscript.

REFERENCES

1. Patel, S., and Latterich, M. (1998) *Trends. Cell Biol.* **8,** 65–71
2. Vale, R. D. (2000) *J. Cell Biol.* **150,** 13–19
3. Ogura, T., and Wilkinson, A. J. (2001) *Genes Cells* **6,** 575–597
4. Woodman, P. G. (2003) *J. Cell Sci.* **116,** 4283–4290
5. Latterich, M., Fröhlich, K. U., and Schekman, R. (1995) *Cell* **82,** 885–893
6. Rabouille, C., Levine, T. P., Peters, J. M., and Warren, G. (1995) *Cell* **82,**

905–914
7. Patel, S. K., Indig, F. E., Olivieri, N., Levine, N. D., and Latterich, M. (1998) *Cell* **92,** 611–620
8. Roy, L., Bergeron, J. J., Lavoie, C., Hendriks, R., Gushue, J., Fazel, A., Pelletier, A., Morre, D. J., Subramaniam, V. N., Hong, W., and Paiement, J. (2000) *Mol. Biol. Cell* **11,** 2529–2542
9. Braun, S., Matuschewski, K., Rape, M., Thoms, S., and Jentsch, S. (2002) *EMBO J.* **21,** 615–621
10. Jarosch, E., Geiss-Friedlander, R., Meusser, B., Walter, J., and Sommer, T. (2002) *Traffic* **3,** 530–536
11. Rabinovich, E., Kerem, A., Fröhlich, K. U., Diamant, N., and Bar-Nun, S. (2002) *Mol. Cell. Biol.* **22,** 626–634
12. Ye, Y., Meyer, H. H., and Rapoport, T. A. (2003) *J. Cell Biol.* **162,** 71–84
13. Hetzer, M., Meyer, H. H., Walther, T. C., Bilbao-Cortes, D., Warren, G., and Mattaj, I. W. (2001) *Nat. Cell Biol.* **3,** 1086–1091
14. Egerton, M., and Samelson, L. E. (1994) *J. Biol. Chem.* **269,** 11435–11441
15. Shirogane, T., Fukada, T., Muller, J. M., Shima, D. T., Hibi, M., and Hirano, T. (1999) *Immunity* **11,** 709–719
16. Pleasure, I. T., Black, M. M., and Keen, J. H. (1993) *Nature* **365,** 459–462
17. Sugita, S., and Sudhof, T. C. (2000) *Biochemistry* **39,** 2940–2949
18. Yamada, T., Okuhara, K., Iwamatsu, A., Seo, H., Ohta, K., Shibata, T., and Murofushi, H. (2000) *FEBS Lett.* **466,** 287–291
19. Zhang, H., Wang, Q., Kajino, K., and Greene, M. I. (2000) *DNA Cell Biol.* **19,** 253–263
20. Joaquin Partridge, J., Lopreiato, J., Latterich, M., and Indig, F. E. (2003) *Mol. Biol. Cell* **14,** 4221–4229
21. Kondo, H., Rabouille, C., Newman, R., Levine, T. P., Pappin, D., Freemont, P., and Warren, G. (1997) *Nature* **388,** 75–78
22. Uchiyama, K., Jokitalo, E., Kano, F., Murata, M., Zhang, X., Canas, B., Newman, R., Rabouille, C., Pappin, D., Freemont, P., and Kondo, H. (2002) *J. Cell Biol.* **159,** 855–866
23. Koegl, M., Hoppe, T., Schlenker, S., Ulrich, H. D., Mayer, T. U., and Jentsch, S. (1999) *Cell* **96,** 635–644
24. Ghislain, M., Dohmen, R. J., Levy, F., and Varshavsky, A. (1996) *EMBO J.* **15,** 4884–4899
25. Hitchcock, A. L., Krebber, H., Frietze, S., Lin, A., Latterich, M., and Silver, P. A. (2001) *Mol. Biol. Cell* **12,** 3226–3241
26. Jarosch, E., Taxis, C., Volkwein, C., Bordallo, J., Finley, D., Wolf, D. H., and Sommer, T. (2002) *Nat. Cell Biol.* **4,** 134–139
27. Meyer, H. H., Shorter, J. G., Seemann, J., Pappin, D., and Warren, G. (2000) *EMBO J.* **19,** 2181–2192
28. Dai, R. M., and Li, C. C. (2001) *Nat. Cell Biol.* **3,** 740–744
29. Nagahama, M., Suzuki, M., Hamada, Y., Hatsuzawa, K., Tani, K., Yamamoto, A., and Tagaya, M. (2003) *Mol. Biol. Cell* **14,** 262–273
30. Yuan, X., Shaw, A., Zhang, X., Kondo, H., Lally, J., Freemont, P. S., and Matthews, S. (2001) *J. Mol. Biol.* **311,** 255–263
31. Uchiyama, K., Jokitalo, E., Lindman, M., Jackman, M., Kano, F., Murata, M., Zhang, X., and Kondo, H. (2003) *J. Cell Biol.* **161,** 1067–1079
32. Decottignies, A., Evain, A., and Ghislain, M. (2004) *Yeast* **21,** 127–139
33. Schuberth, C., Richly, H., Rumpf, S., and Buchberger, A. (2004) *EMBO Rep.* **5,** 818–824
34. Buchberger, A., Howard, M. J., Proctor, M., and Bycroft, M. (2001) *J. Mol. Biol.* **307,** 17–24
35. Rancour, D. M., Dickey, C. E., Park, S., and Bednarek, S. Y. (2002) *Plant Physiol.* **130,** 1241–1253
36. Bar-Peled, M., and Raikhel, N. V. (1996) *Anal. Biochem.* **241,** 140–142
37. Jimenez, C. R., Huang, L., Qin, Y., and Burlingame, A. L. (1998) in *Current Protocols in Protein Science*, pp. 16.14.11–16.14.15, Wiley and Sons, Inc., Edison, NJ
38. Perkins, D. N., Pappin, D. J., Creasy, D. M., and Cottrell, J. S. (1999) *Electrophoresis* **20,** 3551–3567
39. Söllner, T., Bennett, M. K., Whiteheart, S. W., Scheller, R. H., and Rothman, J. E. (1993) *Cell* **75,** 409–418
40. Kang, B.-H., Busse, J. S., Dickey, C., Rancour, D. M., and Bednarek, S. Y. (2001) *Plant Physiol.* **126,** 47–68
41. Hajdukiewicz, P., Svab, Z., and Maliga, P. (1994) *Plant Mol. Biol.* **25,** 989–994
42. Chook, Y. M., Jung, A., Rosen, M. K., and Blobel, G. (2002) *Biochemistry* **41,** 6955–6966
43. Rowlands, M. G., Newbatt, Y. M., Prodromou, C., Pearl, L. H., Workman, P., and Aherne, W. (2004) *Anal. Biochem.* **327,** 176–183
44. Krysan, P. J., Young, J. C., Tax, F., and Sussman, M. R. (1996) *Proc. Natl. Acad. Sci. U. S. A.* **93,** 8145–8150
45. Murashige, T., and Skoog, F. (1962) *Physiol. Plant.* **15,** 473–497
46. Axelos, M., Curie, C., Mazzolini, L., Bardet, C., and Lescure, B. (1992) *Plant Physiol. Biochem.* **30,** 123–128
47. Altschul, S. F., Madden, T. L., Schaffer, A. A., Zhang, J., Zhang, Z., Miller, W., and Lipman, D. J. (1997) *Nucleic Acids Res.* **25,** 3389–3402
48. Bar-Peled, M., and Raikhel, N. V. (1997) *Plant Physiol.* **114,** 315–324
49. Song, C., Wang, Q., and Li, C. C. (2003) *J. Biol. Chem.* **278,** 3648–3655
50. Feiler, H. S., Desprez, T., Santoni, V., Kronenberger, J., Caboche, M., and Traas, J. (1995) *EMBO J.* **14,** 5626–5637
51. Peters, J. M., Walsh, M. J., and Franke, W. W. (1990) *EMBO J.* **9,** 1757–1767
52. Peters, J. M., Harris, J. R., Lustig, A., Muller, S., Engel, A., Volker, S., and Franke, W. W. (1992) *J. Mol. Biol.* **223,** 557–571
53. Rouiller, I., Butel, V. M., Latterich, M., Milligan, R. A., and Wilson-Kubalek, E. M. (2000) *Mol. Cell* **6,** 1485–1490
54. Zhang, X., Shaw, A., Bates, P. A., Newman, R. H., Gowen, B., Orlova, E., Gorman, M. A., Kondo, H., Dokurno, P., Lally, J., Leonard, G., Meyer, H., van Heel, M., and Freemont, P. S. (2000) *Mol. Cell* **6,** 1473–1484
55. Lamb, J. R., Fu, V., Wirtz, E., and Bangs, J. D. (2001) *J. Biol. Chem.* **276,** 21512–21520
56. Rockel, B., Jakana, J., Chiu, W., and Baumeister, W. (2002) *J. Mol. Biol.* **317,** 673–681
57. Rouiller, I., DeLaBarre, B., May, A. P., Weis, W. I., Brunger, A. T., Milligan, R. A., and Wilson-Kubalek, E. M. (2002) *Nat. Struct. Biol.* **9,** 950–957
58. Beuron, F., Flynn, T. C., Ma, J., Kondo, H., Zhang, X., and Freemont, P. S. (2003) *J. Mol. Biol.* **327,** 619–629
59. DeLaBarre, B., and Brunger, A. T. (2003) *Nat. Struct. Biol.* **10,** 856–863
60. Huyton, T., Pye, V. E., Briggs, L. C., Flynn, T. C., Beuron, F., Kondo, H., Ma, J., Zhang, X., and Freemont, P. S. (2003) *J. Struct. Biol.* **144,** 337–348
61. Dreveny, I., Kondo, H., Uchiyama, K., Shaw, A., Zhang, X., and Freemont, P. S. (2004) *EMBO J.* **23,** 1030–1039
62. Roggy, J. L., and Bangs, J. D. (1999) *Mol. Biochem. Parasitol.* **98,** 1–15
63. Wang, Q., Song, C., and Li, C. C. (2003) *Biochem. Biophys. Res. Commun.* **300,** 253–260
64. Dalal, S., Rosser, M. F., Cyr, D. M., and Hanson, P. I. (2004) *Mol. Biol. Cell* **15,** 637–648
65. Rape, M., Hoppe, T., Gorr, I., Kalocay, M., Richly, H., and Jentsch, S. (2001) *Cell* **107,** 667–677
66. Ye, Y., Meyer, H. H., and Rapoport, T. A. (2001) *Nature* **414,** 652–656
67. Meyer, H. H., Wang, Y., and Warren, G. (2002) *EMBO J.* **21,** 5645–5652
68. Flierman, D., Ye, Y., Dai, M., Chau, V., and Rapoport, T. A. (2003) *J. Biol. Chem.* **278,** 34774–34782
69. Yuan, X., Simpson, P., Kondo, H., McKeown, C., Dreveny, I., Zhang, X., Freemont, P. S., and Matthews, S. (2004) *J. Biomol. NMR* **28,** 309–310
70. Fröhlich, K. U., Fries, H. W., Rudiger, M., Erdmann, R., Botstein, D., and Mecke, D. (1991) *J. Cell Biol.* **114,** 443–453
71. Madeo, F., Schlauer, J., Zischka, H., Mecke, D., and Fröhlich, K. U. (1998) *Mol. Biol. Cell* **9,** 131–141
72. Beemster, G. T., Fiorani, F., and Inzé, D. (2003) *Trends Plant Sci.* **8,** 154–158
73. Beemster, G. T., and Baskin, T. I. (1998) *Plant Physiol.* **116,** 1515–1526
74. Riou-Khamlichi, C., Menges, M., Healy, J. M., and Murray, J. A. (2000) *Mol. Cell. Biol.* **20,** 4513–4521
75. Chenna, R., Sugawara, H., Koike, T., Lopez, R., Gibson, T. J., Higgins, D. G., and Thompson, J. D. (2003) *Nucleic Acids Res.* **31,** 3497–3500
76. Thompson, J. D., Higgins, D. G., and Gibson, T. J. (1994) *Nucleic Acids Res.* **22,** 4673–4680